DEEP FLAW DETECTION WITH GIANT MAGNETORESISTIVE (GMR) BASED SELF-NULLING PROBE

Buzz Wincheski and Min Namkung
NASA Langley Research Center
Hampton, VA 23681

INTRODUCTION

The use of giant magnetoresistive (GMR) sensors for electromagnetic nondestructive evaluation has grown considerably in the last few years [1-4]. Technological advances in the research and development of giant magnetoresistive materials has led to commercially available GMR sensors with many qualities well suited for electromagnetic NDE. Low cost GMR magnetometers are now available which are highly sensitive to the magnitude of the external magnetic field, have a small package size, consume little power, and operate at room temperature [5]. Incorporation of these sensors into electromagnetic NDE probes has widened the application range of the field. In particular, the low frequency sensitivity of the devices provides a practical means to perform electromagnetic inspections on thick layered conducting structures.

The incorporation of a commercially available GMR sensor into the Self-Nulling Probe has been explored in the past [3]. This research showed that the modification could be performed in a straightforward manner to greatly enhance the low frequency capabilities of the device. A limiting factor in this previous work appeared to be the increased background level with decreasing frequency for flaw detection at depths greater than approximately 5 mm.

In order to improve the signal to noise ratio of the GMR based Self-Nulling Probe the incorporation of active feedback in the probe design has been investigated. The active feedback is shown to greatly reduce the background field levels in the interior of the probe where the GMR sensor is housed. This, combined with image processing to filter out background variations from the processed data, has resulted in a greatly improved signal to noise ratio for very deeply buried flaws in conducting materials.

ELECTROMAGNETIC INSPECTION OF THICK ALUMINUM COMPONENTS

Electromagnetic inspection of thick conducting materials requires a low frequency excitation, due to the skin depth relationship [6,7] which is given in CGS units by

$$B_z = B_0 \exp(-z/\delta), \tag{1}$$

$$\delta = c \Big/ \sqrt{2\pi\mu\omega\sigma}, \tag{2}$$

where B_z is the magnetic field at depth z into the material under test, B_0 is the magnetic field at the surface, c is the speed of light, μ is the permeability, ω is the angular frequency, σ is the conductivity, and δ is the skin depth. The skin depth of a highly conducting material will be quite small unless the frequency of operation is also lowered. In order for the skin depth to reach 1 centimeter in an aluminum alloy with μ=1 and σ=1.7 x 10^{17} sec^{-1}, for example, the operating frequency must be reduced to 130 Hz.

As explained above, an eddy current device designed for deep inspections must be sensitive to low frequency magnetic fields. Pickup coil type sensors, however, become ineffective in this frequency range due to Faraday's law of electromagnetic induction which states

$$\varepsilon = -\frac{A}{c}\frac{dB}{dt} \propto \omega \sin \omega t . \qquad (3)$$

The electromotive force, ε, induced around a circuit is proportional to area enclosed, A, multiplied by the time rate of change of the magnetic field through the circuit [6]. Since the output of the coil is proportional to the time rate of change of the magnetic field the effectiveness of the inspection decreases with decreasing frequency.

Giant magneto-resistive sensors respond to the magnitude of the external field instead of the time rate of change of the field and therefore do not lose sensitivity at low frequencies. In the absence of an applied field, the resistivity of the GMR element is high due to scattering between oppositely polarized electrons in the antiferromagnetically coupled multi-layers of the device. An external field aligns the magnetic moments of the ferromagnetic layers, eliminating this scattering mechanism and thereby reducing the resistivity of the material [5]. A schematic diagram of a commercially available GMR sensor is displayed in figure 1. In this design four GMR elements are arranged in a Wheatstone bridge configuration on an eight-pin integrated circuit.

Figure 2 shows the calibration data for the GMR sensor displayed schematically in figure 1 [3]. This data was acquired with the sensor placed in the center of a Helmholtz pair driven by a precision current source. Fifteen volts were placed across the GMR bridge, and a 20 dB differential preamplifier was used to amplify the output voltage of the sensor. Note that the output increases with the magnitude of the magnetic field and that the sensitivity, the slope of the output voltage versus applied field, drops dramatically in the low field region between approximately ± 0.5 Oe.

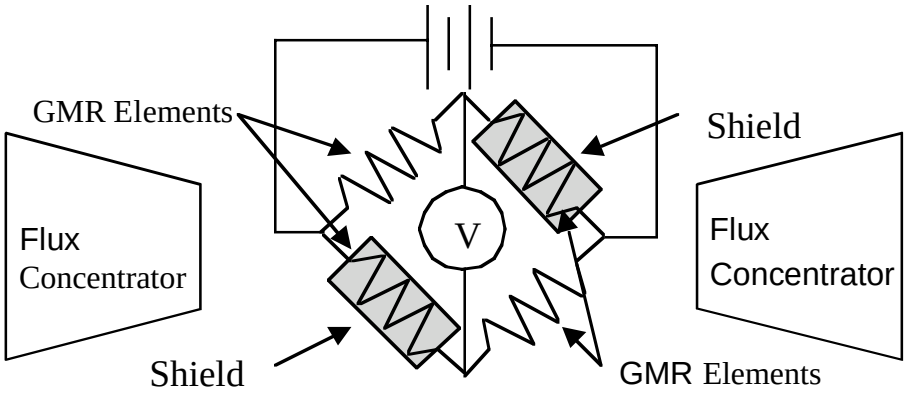

Figure 1. Schematic diagram of commercially available GMR sensor [5].

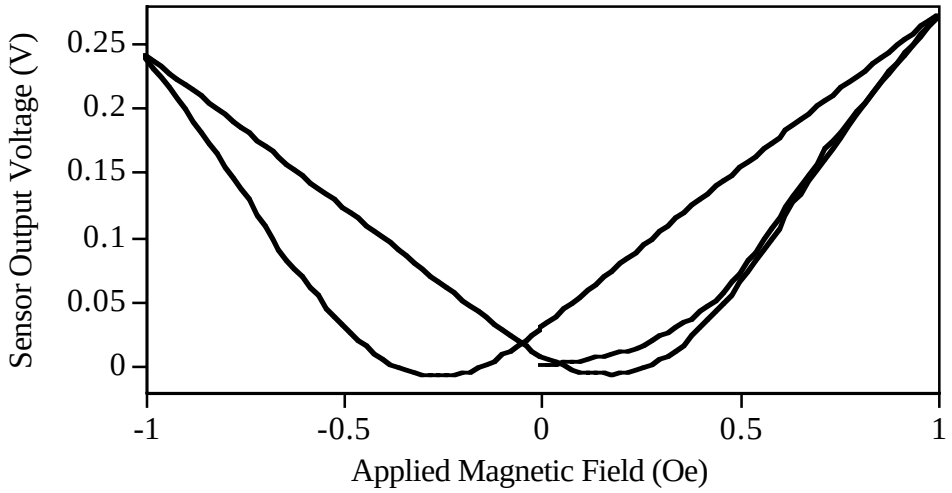

Figure 2. Calibration data for GMR sensor [3].

GMR BASED SELF-NULLING PROBE WITH ACTIVE FEEDBACK

A schematic diagram of the GMR based Self-Nulling Probe including the active feedback circuit is shown in figure 3. The design is based upon the NASA LaRC developed Self-Nulling Eddy Current Probe for surface and near surface flaw detection [8]. The new probe has two main design changes from the original Self-Nulling Eddy Current Probe. A GMR sensor is used in place of a pickup coil as the field sensor and a second current source is added to provide active feedback to the GMR sensor location.

The use of active feedback inside the flux-focusing lens enables a complete cancellation of the sinusoidal stray fields at the GMR sensor location. Previous work has shown that at low frequencies the magnetic flux leakage around the bottom of the flux focusing lens results in a large background signal level [3,9]. In the current design the background signal is removed by applying a feedback signal at the same frequency as the drive source but 180° out of phase with sensor output to the feedback coil. The feedback coil is also used to shift the operating point of the GMR sensor out of the low field region where the sensitivity of the device is low. For this a DC voltage is applied to the feedback coil to provide a static background field level of approximately 0.75 Oe.

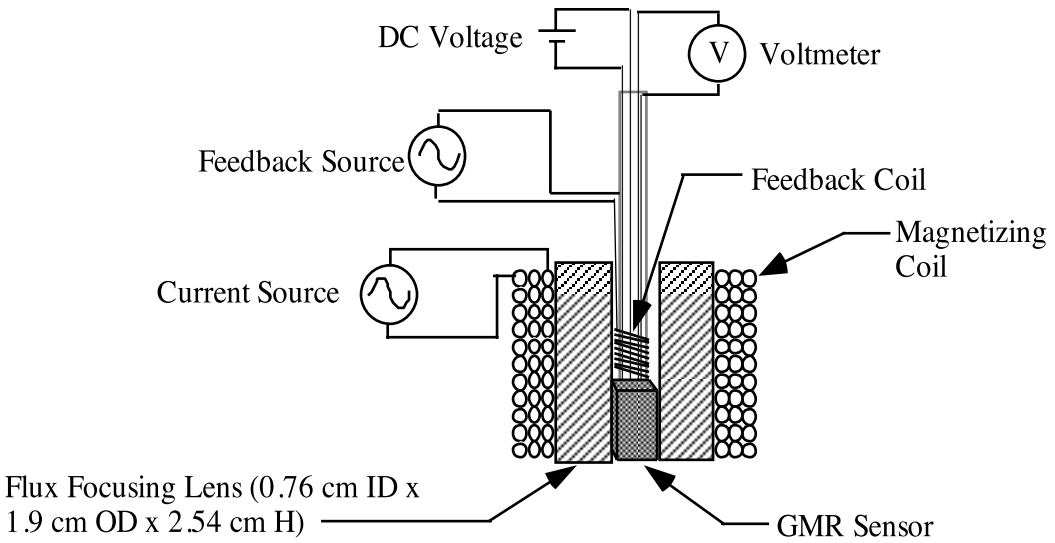

Figure 3. Schematic diagram of GMR based Self-Nulling Probe with active feedback.

Figure 4 displays the drive coil and sensor output waveforms for the GMR based Self-Nulling Probe at various stages of feedback to the GMR sensor. The data were acquired at 185 Hz drive with 15 volts to the GMR bridge and 40 dB preamplification. The waveforms in the figure 4a were taken without any feedback. As was seen in previous work, the output signal is rectified due to the insensitivity of the GMR sensor to the direction of the applied field [3]. A significant drop in the output voltage is observed when the probe is placed on the conducting sample, although a relatively large output voltage is still observed.

Figure 4b displays the change in the output as the feedback source is adjusted. With the probe on the sample the application of a DC bias to the feedback coil shifts the operating point of the sensor away from the zero crossing area and up the calibration curve to a location of higher sensitivity. This results in an increased output amplitude of the sensor, as is seen in the right hand plot. Also note that the signal is now at the same frequency as the drive source, with the rectification of the signal eliminated. The final step is then to apply a sinusoidal signal to the feedback coil at the drive coil frequency but 180° out of phase with the probe output. The resulting probe output is a DC shifted amplitude with only a very small AC component. Adjusting the feedback in this manner cancels the leakage magnetic fields in the center of the probe and biases the sensor in order to obtain maximum sensitivity to small changes in the magnetic field caused by deeply buried defects.

EXPERIMENTAL RESULTS

Once the feedback source is adjusted as described above and illustrated in figure 4b the sample under test can be scanned. A lock-in amplifier referenced to the drive coil is used to record both the amplitude and phase of the probe output as a function of position on the sample surface. The first sample tested was a two-layer aluminum alloy lay-up, as shown in figure 5. The top layer was formed of an unflawed 4.76 mm thick plate. The lower layer was formed from a 1 mm thick aluminum plate with fatigue cracks grown from either side of a drilled center hole. The sample was scanned from the unflawed side with the probe operating at 375 Hz.

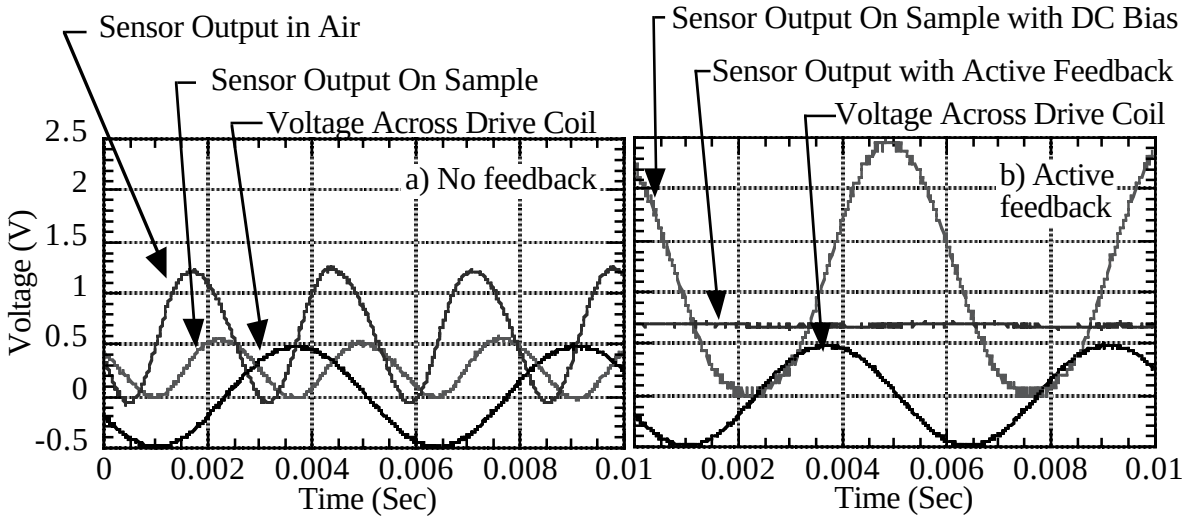

Figure 4. Drive coil and probe output waveforms at various stages of active feedback to the GMR sensor.

Figure 5 displays the geometry and a surface plot of the experimentally measured probe output amplitude for the first experimental sample. The edge of the bottom plate, center hole, and fatigue cracks emanating from either side of the hole are all clearly visible in the surface plot. In addition, a peak in the output amplitude at the location of the fatigue crack tips is evident in the data. This feature, due to the detailed nature of the perturbed current path around the flaw, has been extensively studied in the past for surface flaw detection with the Self-Nulling Probe [10]. The detection of this maximum field amplitude at the crack tip for deeply buried flaws illustrates the detail that can be obtained with the GMR based Self-Nulling Probe incorporating active feedback.

A second experimental sample was fabricated to examine the detection capabilities of the probe for flaws at varying depths in thick layered conductors such as airframe wings. A set of thirteen, 1 mm thick, aluminum plates with a cross section of 15 x 15 cm^2 was obtained. An EDM notch of 1.4 x 0.0127 cm^2 was placed in the center of one of the plates. The location of this flawed layer within the stack of unflawed plates could then be varied, and data acquired over the flawed area for each case. Previous results using the GMR Self-Nulling Probe without the feedback coil showed that the flaw could be clearly detected in the 6^{th} and 7^{th} layer, but that the signal to noise ratio dropped dramatically for deeper layers [3].

The capabilities of the modified sensor along with a schematic representation of the sample are shown in figure 6. The plotted data were acquired at an operating frequency of 185 Hz with the flaw placed in the 10^{th} layer of the sample, beneath 9 mm of unflawed aluminum. The flaw location is clearly imaged in the experimental data. A double peak indication is detected since the notch length of 1.4 cm is less than the outside diameter of the GMR based Self-Nulling Probe (1.9 cm). A peak in the output is observed when the probe is centered over either tip of the flaw. When the probe is centered over the midpoint of the notch, however, the majority of the induced current will flow unperturbed around the flaw tips.

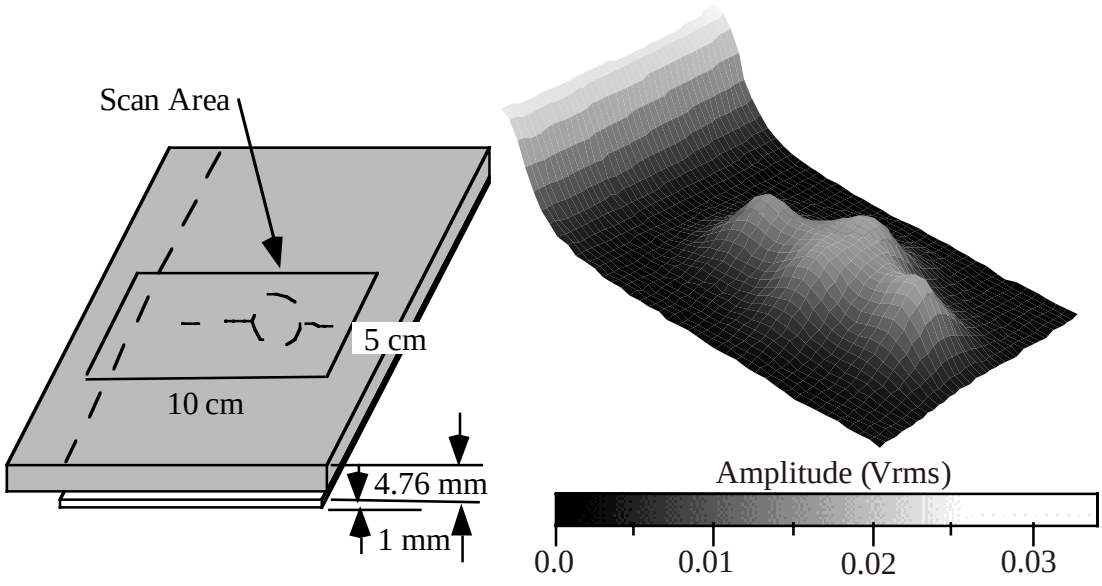

Figure 5. Sample geometry and surface plot of experimental data for fatigue crack detection through 4.76 mm unflawed aluminum alloy plate.

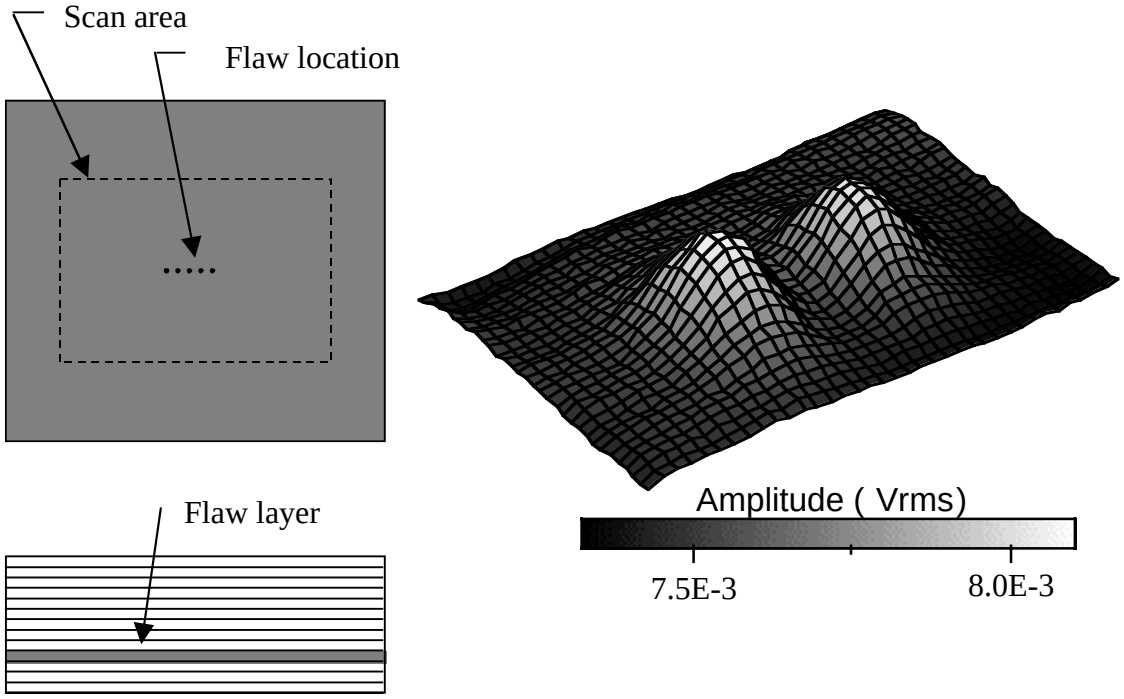

Figure 6. Sample geometry and surface plot of experimental data for 1.4 cm long EDM notch in 10th of 13 1.0 mm thick aluminum alloy plates.

The results shown above for the 10th layer flaw were achieved by using some additional data analysis and image processing that were not required for shallower flaws such as that depicted in figure 5. In figure 5 the amplitude of the probe output voltage was used to identify the flaw location. In figure 6, however, the amplitude data was combined with the phase information in order to obtain a phase rotated amplitude. The probe output voltage was calculated as

$$V_{out} = A\,\mathrm{Cos}(\varphi + \beta) \qquad (4)$$

were V_{out} is the probe output voltage, A is the root mean square output amplitude, φ is the phase of the output waveform with reference to the drive signal, and β is a constant phase shift applied uniformly to all data points. The phase shift is rotated so as to minimize output voltage changes due to lift-off effects and maximize the signal due to the deeply buried flaws. The method is very similar to the standard eddy current practice of rotating the impedance plane diagram so as to provide a horizontal signal for lift-off variations and then monitoring the vertical component of the change in impedance.

After the amplitude and phase data were combined a simple image processing routine was used to enhance the image quality for greater flaw detectability. The image was first flattened in order to remove any linear drift in the data caused by the presence of a small angle between the scanning plane and the sample surface or electronics drift during the scan. A low pass two-dimensional Fourier filter was then applied across the sample set in order to remove any high frequency noise caused by the scanning system. Figure 7 details the data analysis and image processing steps as applied to the data presented in figure 6.

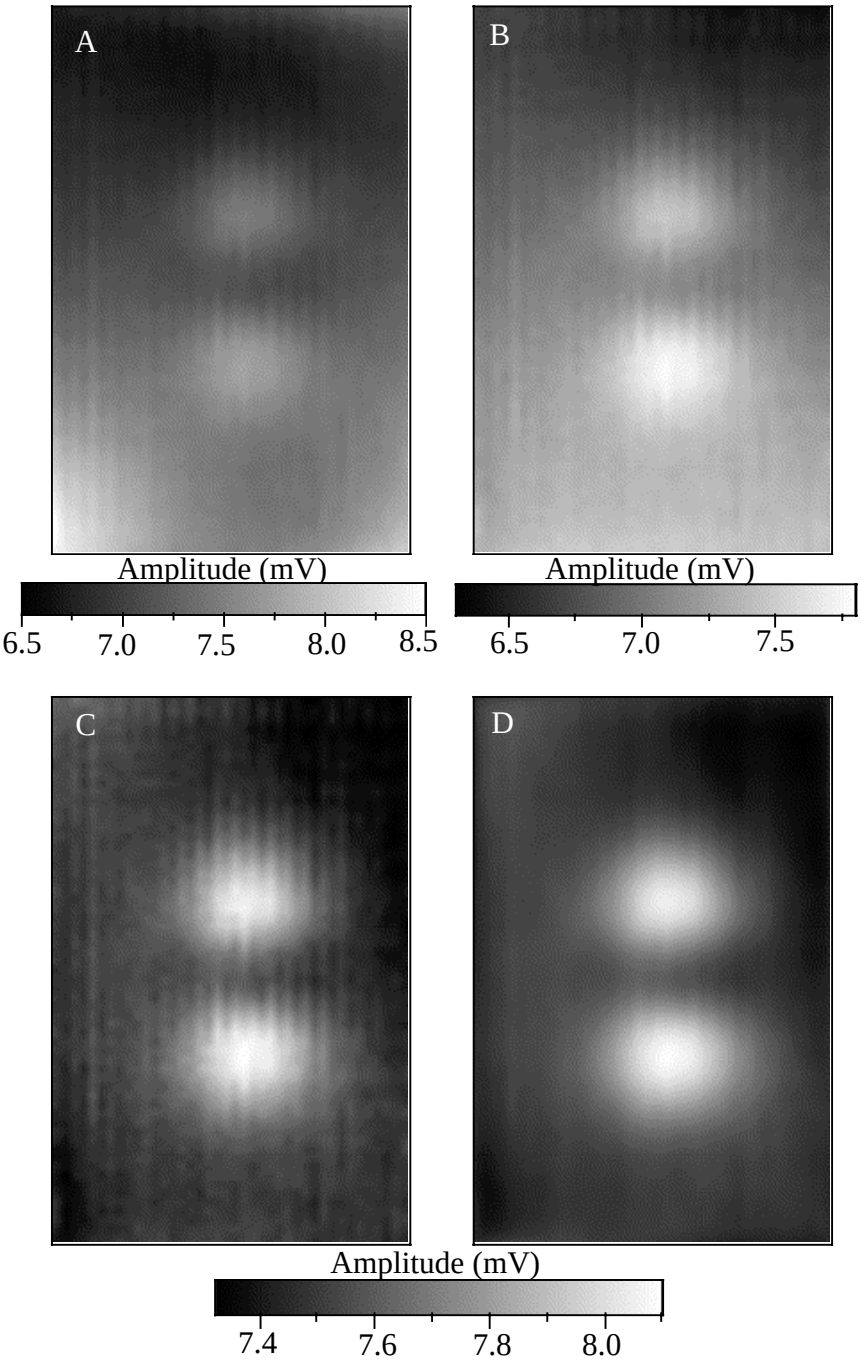

Figure 7. Data analysis and image processing steps for 1cm deep flaw; (A) sensor output amplitude, (B) phase rotated amplitude, (C) flattened image, (D) low pass Fourier filtered data.

SUMMARY

In this paper a design modification to the Very-Low Frequency GMR Based Self-Nulling Probe has been presented to enable improved signal to noise ratio for deeply buried flaws. The design change consists of incorporating a feedback coil in the center of the flux focusing lens. The use of the feedback coil enables cancellation of the leakage fields in the center of the probe and biasing of the GMR sensor to a location of high magnetic field sensitivity. The effect of the feedback on the probe output was examined, and experimental results for deep flaw detection were presented. The experimental results

show that the modified probe is capable of clearly identifying flaws up to 1 cm deep in aluminum alloy structures.

REFERENCES

1. W. F. Arvin, *Review of Progress in QNDE*, Vol. 15, 1145, Plenum Press, New York, 1996.
2. E.S. Boltz and T.C. Tiernan, *Review of Progress in QNDE*, Vol. 17, 1033, Plenum Press, New York, 1998.
3. B. Wincheski and M. Namkung, *Review of Progress in QNDE*, Vol. 18, 1177, Plenum Press, New York, 1999.
4. M. Namkung, B. Wincheski, S. Nath, and J. Fulton, *in current proceedings.*
5. *NVE Sensor Engineering and Application Notes*, Nonvolatile Electronics, INC., 1997.
6. J.D. Jackson, *Classical Electrodynamics*, pp. 210, 296-298, John Wiley &Sons, 1975.
7. H.L. Libby, *Introduction to Electromagnetic Nondestructive Test Methods*, John Wiley & Sons, 1971.
8. B. Wincheski, J.P. Fulton, S. Nath, M. Namkung, and J.W. Simpson, "Self-Nulling Eddy Current Probe for Surface and Subsurface Flaw Detection," *in Materials Evaluation*, Vol. 52/Number 1 (January 1994).
9. B. Wincheski, M. Namkung, J. Fulton, and S. Nath, *Review of Progress in QNDE*, Vol. 13B, 1611, Plenum Press, New York, 1994.
10. M. Namkung, J.P. Fulton, B. Wincheski, and C.G. Clendenin, *Review of Progress in QNDE*, Vol. 13B, 1633, Plenum Press, New York, 1994.